

Accepted Manuscript

Analysis of bioethanol samples through Inductively Coupled Plasma Mass Spectrometry with a total sample consumption system

Carlos Sánchez, Charles-Philippe Lienemann, Jose-Luis Todolí

PII: S0584-8547(16)30153-7
DOI: doi: [10.1016/j.sab.2016.08.018](https://doi.org/10.1016/j.sab.2016.08.018)
Reference: SAB 5122

To appear in: *Spectrochimica Acta Part B: Atomic Spectroscopy*

Received date: 17 March 2016
Revised date: 19 July 2016
Accepted date: 14 August 2016

Please cite this article as: Carlos Sánchez, Charles-Philippe Lienemann, Jose-Luis Todolí, Analysis of bioethanol samples through Inductively Coupled Plasma Mass Spectrometry with a total sample consumption system, *Spectrochimica Acta Part B: Atomic Spectroscopy* (2016), doi: [10.1016/j.sab.2016.08.018](https://doi.org/10.1016/j.sab.2016.08.018)

This is a PDF file of an unedited manuscript that has been accepted for publication. As a service to our customers we are providing this early version of the manuscript. The manuscript will undergo copyediting, typesetting, and review of the resulting proof before it is published in its final form. Please note that during the production process errors may be discovered which could affect the content, and all legal disclaimers that apply to the journal pertain.



Analysis of bioethanol samples through
Inductively Coupled Plasma Mass Spectrometry
with a total sample consumption system

Carlos Sánchez,^a Charles-Philippe Lienemann,^b Jose-Luis Todolí^{a*}

^aDepartment of Analytical Chemistry, Nutrition and Food Sciences, P.O. Box 99, 03080, Alicante, Spain.

^bIFP Energies Nouvelles, Rond-point de l'échangeur de Solaize, BP 3, F-69360 Solaize, France

Abstract

Bioethanol real samples have been directly analyzed through ICP-MS by means of the so called High Temperature Torch Integrated Sample Introduction System (hTISIS). Because bioethanol samples may contain water, experiments have been carried out in order to determine the effect of ethanol concentration on the ICP-MS response. The ethanol content studied went from 0 to 50%, because higher alcohol concentrations led to carbon deposits on the ICP-MS interface. The spectrometer default spray chamber (double pass) equipped with a glass concentric pneumatic micronebulizer has been taken as the reference system. Two flow regimes have been evaluated: continuous sample aspiration at $25 \mu\text{L min}^{-1}$ and $5 \mu\text{L}$ air-segmented sample injection. hTISIS temperature has been shown to be critical, in fact ICP-MS sensitivity increased with this variable up to $100 - 200 \text{ }^\circ\text{C}$ depending on the solution tested. Higher chamber temperatures led to either a drop in signal or a plateau. Compared with the reference system, the hTISIS improved the sensitivities by a factor included within the 4 to 8 range while average detection limits were 6 times lower for the latter device. Regarding the influence of the ethanol concentration on sensitivity, it has been observed that an increase in the temperature was not enough to eliminate the interferences. It was also necessary to modify the torch position with respect to the ICP-MS interface to overcome them. This fact was likely due to the different extent of ion plasma radial diffusion encountered as a function of the matrix when working at high chamber temperatures. When the torch was moved 1 mm plasma down axis, ethanolic and aqueous solutions provided statistically equal sensitivities. A preconcentration procedure has been applied in order to validate the methodology. It has been found that, under optimum conditions from the point of view of matrix

effects, recoveries for spiked samples were close to 100%. Furthermore, analytical concentrations for real samples following the preconcentration method and the direct determination were not significantly different. The quantification method was finally based on external calibration with standards containing 50% (v/v) ethanol content.

Keywords:

Bioethanol; Metals; ICP-MS; High-Temperature torch integrated sample introduction system (hTISIS).

1. Introduction

Bioethanol is considered as a promising alternative to fossil fuels [1,2] and in its anhydrous form it is often blended to products such as gasoline thus giving rise to the so-called ethanol fuel. Nevertheless, this product may contain organic as well as inorganic pollutants, among them metals and metalloids [3]. The presence of these species may result detrimental from the point of view of engine performance and environmental quality. Although official methods have been developed to determine the metal and metalloid content in fossil fuels, a few methods exist in the case of ethanol fuel [4,5,6]. So far, there are only procedures for determining the content of Na, K, Ca, Mg, Fe, Cu, P and S in this kind of samples and no attention is paid to other heavy toxic metals.

Several spectrometric techniques have been employed to perform this kind of analysis. Recently, High Resolution Continuum Source Flame Atomic Absorption Spectrometry was applied to the sequential determination of nine metals in ethanol fuel samples [7]. Due to the low metal content usually present in bioethanol samples (*i.e.*, $\mu\text{g L}^{-1}$), Inductively Coupled Plasma Mass Spectrometry (ICP-MS) appears as an excellent alternative to other spectrometric atomic absorption and emission techniques. However, some problems can be found when only bioethanol containing samples are introduced into the plasma. In fact, in its hydrated form, bioethanol may contain up to 7% of water. Moreover, the fermented solution present before the distillation step may contain ethanol volume percentages ranging from 12 to 15%. In addition, as much as 300 different organic compounds such as longer chain alcohols, ketones or aldehydes may be present in the matrix [1]. This may cause degradation in

the accuracy of the determination if the matrix nature is not considered [6]. Obviously, the introduction of an organic specimen into the plasma induces severe ICP-MS spectral interferences thus making it difficult to quantify analytes such as ^{28}Si or ^{52}Cr [8]. An additional difficulty is that there are limited certified reference materials what hampers the method validation procedure [1,2].

Studies trying to overcome some of these problems have been published based on the use of collision or reaction cells [9], dedicated sample introduction systems such as Electrothermal Vaporization [10], micronebulization [11] or flow injection [12]. Recently, Virgilio *et al.* proposed a method based on the use of ICP-MS/MS to carry out ethanol fuel analysis. In this methodology, samples were diluted with a nitric acid solution and matrix matching was employed for elemental quantification [13].

Non spectral interferences can be overcome by using well known methods such as sample dilution with water [14], matrix matching [15] or internal standardization [16]. All these procedures suffer from their own drawbacks such as loss in sensitivity, time consumption or the lack of appropriate elements to be used as internal standard. In a recent report, it was verified that it is possible to perform bioethanol analysis in ICP-OES by means of a high temperature total sample consumption system [17]. The basic principle of the so-called High Temperature Torch Integrated Sample Introduction System (hTISIS) consists of the complete aerosol evaporation before it enters the plasma. In this manner, analyte transport efficiency is virtually 100% regardless the sample matrix. Therefore, interferences originated in the sample introduction system are removed. In order to avoid plasma degradation caused by the introduction of organic matter, air segmented 5 μL injection or low liquid flow rates are employed [18]. Additional advantages of the hTISIS over conventional sample

introduction systems include improved sensitivities and limits of detection and shorter wash out times.

So far, most of the existing studies have been focused on the analysis of ethanol fuel. The aim of the present work was thus to test the combination of hTISIS-ICP-MS as a rapid and direct way for performing multielemental determination in bioethanol samples. In a first step, analytical figures of merit were evaluated. Additional problems caused by the introduction of organic samples in ICP-MS such as non-spectral interferences were discussed and characterized. All the studies were done following two different flow regimes: (i) continuous sample aspiration at a 25 $\mu\text{L min}^{-1}$ liquid flow rate, and; (ii) air-segmented (5 μL) injection mode.

2. Experimental

2.1. Solutions and samples

Standards containing ethanol at concentrations ranging from 0 to 50 % (v/v) were prepared using ultrapure water ($R < 18.2 \text{ M}\Omega$) obtained with a Millipore water purification system (El Paso, TX, USA) and analytical grade ethanol 96% (Panreac, Barcelona, Spain). Multielemental standards were obtained from a stock solution (Merck IV, Darmstadt, Germany). Blanks containing variable ethanol and water concentrations were also prepared. All these synthetic solutions were filtered with a 0.45 μm PTFE filter pore size (Filabet, Barcelona, Spain).

Twenty-eight real samples containing water concentrations from 0 to 45% were analyzed. These samples were 1:1 (v/v) diluted with ultrapure water ($R < 18.2 \text{ M}\Omega$) and

the standards used for elemental quantification were prepared in a 1:1 (v/v) ethanol/water matrix. Recovery studies were performed in which the diluted samples were spiked to $250 \mu\text{g L}^{-1}$ by using a Merck IV multielemental stock solution. In this case, non spiked samples were taken as blanks.

Viscosity was obtained with an Ostwald viscometer employing ultrapure water as the reference solvent. For the tested real samples, this physical property ranged from 1.24 to 2.19 mPa s^{-1} . In order to measure the surface tension 30 drops provided by a peristaltic pump under controlled conditions were recovered in a polyethylene container and further weighed. The final value of this property was obtained using ultrapure water as reference solvent. Surface tension was included within the 20.9 to 27.5 mN m^{-1} range depending on the sample considered.

Real samples corresponded to bioethanol produced from beet (labeled as B9 to B16 and B19-B23), wheat (B2, B5, B7 and B17) and finally from sugarcane (B4) and wine (B18). Together with all these samples, an ethanol sample containing additives (B3) was also analyzed.

2.2. Instrumentation

An Agilent Technologies 7700x ICP-MS spectrometer (Santa Clara, California, USA) equipped with a high matrix introduction system (HMI) was employed to take the ionic intensities of the analytes shown in Table 1. A hTISIS equipped with a 9 cm^3 single-pass spray chamber was adapted to the spectrometer. The operating conditions are also gathered in Table 1. A glass pneumatic concentric nebulizer, TR-50-C0.5 (Meinhard Glass Products, Santa Ana, USA) was employed. Strictly speaking this is not considered

as a 'micro nebulizer', however it was able to work in a stable fashion, thus leading to satisfactory analytical figures of merit, when liquid flow rates on the order of tens of microliters per minute were selected.

The solutions were delivered to the nebulizer by means of a peristaltic pump (Perimax 16 antiplus, Spetec) and a 0.19-mm id flared end PVC-based tubing (Glass Expansion, Melbourne, Australia) was employed. In the air segmented injection mode, the peristaltic pump continuously aspirated air. A given sample volume was measured with an automatic pipette (Eppendorf, Hamburg, Germany). Then, the nozzle was adapted to the flared end tubing and the solution was aspirated. The sample plug was driven to the nebulizer thus avoiding sample dispersion, as the carrier stream was simply air.

3. Results and Discussion

3.1. Analyte transport efficiency

Experiments were performed in order to verify the impact of the chamber temperature and ethanol content on the mass of analyte leaving the single-pass spray chamber. To achieve this goal, twenty 5 μL standard (200 mg L^{-1} multielemental solution) volumes were consecutively injected and delivered to the nebulizer under the liquid aspiration conditions and nebulizer gas flow rate indicated in Table 1. The aerosol was collected on the surface of a 0.45 μm pore diameter nylon filter inserted into a polycarbonate holder. A vacuum pump was adapted at the exit of the holder and forced the aerosol to pass through this filter. Once the aerosol trapping was

completed, the analyte was extracted in a 2% nitric acid solution. The resulting solutions were analyzed through ICP-MS and the obtained elemental concentration was directly related to the mass of analyte that effectively left the spray chamber (W_{tot}). The experiments were performed for three different ethanol contents (0, 25 and 50%, v/v). At room temperature, W_{tot} for water was three times lower than for the 50% ethanol solution, thus revealing a very important matrix effect in terms of aerosol transport towards the plasma. Figure 1 shows the W_{tot} values found for water and 25% ethanol solution normalized with respect to those encountered for the 50% ethanol solution. This figure reveals that, the higher the chamber temperature, the closer the relative W_{tot} to the unity. Thus, at temperatures above 300°C W_{tot} was similar regardless the ethanol content. Therefore, heating the chamber walls while keeping the sample consumption at a low level was an effective way for overcoming interferences caused by ethanol solutions.

3.2. Analytical figures of merit

3.2.1. Air-segmented injection mode

One of the advantages of the hTISIS is that it is perfectly adapted to the analysis of a few sample microliters. Besides the mitigation of plasma degradation problems, this allows to perform air segmentation. This flow regime eliminates the sample dispersion observed when a liquid carrier stream is used, furthermore, as the spray chamber walls are kept dry between two consecutive injections, sensitivities increase whereas memory effects and wash time decrease. Finally, air is aspirated by the pump

between injections thus mitigating the soot deposition on the surface of the sampler cone. This latter point, together with the High Matrix Introduction (HMI) device of the ICP-MS employed made it possible to introduce 50% (v/v) ethanolic solutions with carbon deposition neither on the torch/injector nor on the ICP-MS interface.

Under the operating conditions selected in the present work, around 30 points were obtained per transient signal what yielded a peak height RSD generally lower than 5% (n=5). The injected sample volume was varied and it was observed that 2.5, 5 and 10 μL provided similar peak heights. This fact revealed the high efficiency of the hTISIS as a liquid sample introduction system for ICP-MS. More interestingly, it was observed that the peak area linearly varied with the injected volume thus making it possible to perform a calibration by merely increasing the introduced volume of a single standard [19].

Figure 2 shows the effect of the hTISIS temperature on the ICP-MS sensitivity. The results are compared against those provided by a conventional double pass spray chamber corresponding to the ICP-MS default sample introduction system. The beneficial effect of the temperature on sensitivity was clearly noticed. In fact an increase in this variable from about 25°C (room temperature) to 100°C led to a 4-fold and 3-fold increase in the peak height for 50% ethanol solution and water, respectively. Above 100°C a decrease in ionic intensity was found that was more significant for ethanol solutions (up to a 50%) than for water (10%). The trends were not correlated with the isotope selected. It is worth mentioning that the enhancement in sensitivity caused by an increase in the hTISIS temperature was lower in ICP-MS than in ICP-OES [17], likely due to phenomena related to the ICP-MS interface that will be further discussed in the present paper.

The data reported in Figure 2 also revealed that the hTISIS improved the sensitivity with respect to a conventional spray chamber. In this case, the improvement factor ranged from 6 to 10. This benefit was specially interesting for bioethanol samples that contained fairly low analyte concentrations.

Limits of detection were calculated according to the $3 s_b/m$ criterion, where s_b corresponded to the standard deviation of twenty consecutive background measurements and m was the slope of the calibration line obtained from five 50% (v/v) ethanol standards. Table 2 gathers the LODs obtained for several isotopes, the double pass spray chamber and the hTISIS operated at two different temperatures. For most of the cases, it was found that, even at room temperature, the hTISIS lowered the LODs with respect to the double pass spray chamber. This was likely due to the improvement in the sensitivity shown for 50% ethanol solutions (see Figure 2). It is also worth mentioning that the increase in the hTISIS temperature led to limits of detection similar to or slightly lower than those found for the hTISIS at room temperature. This was observed despite the degradation in the background stability found as the chamber walls temperature raised. The maximum LODs improvement factors incorporated by the hTISIS with respect to the reference chamber were included within the 10 to 20 range (see ^{208}Pb , ^{209}Bi , ^{107}Ag , ^{59}Co or ^{11}B in Table 2).

3.2.2. Continuous sample aspiration mode

Most analytical methods and standards are based on the continuous introduction of liquid samples into the spectrometer at a given flow rate. This regime was also

evaluated in the present work to compare the results against those previously shown for discrete sample introduction.

As expected, an increase in the hTISIS temperature yielded a grow in ICP-MS sensitivity. Thus, for plain water solutions, at 400°C the ionic signal was from two (^{66}Zn , ^{44}Ca) to five (^{208}Pb , ^{111}Cd , ^{88}Sr , ^{59}Co , ^{55}Mn) times higher as compared to the values registered at room temperature. This was clearly a consequence of the increased mass of analyte reaching the plasma. The situation found for ethanol solutions was somewhat different, as a 2 times average signal improvement was found when the chamber walls temperature increased from around 25°C to 400°C. In this case, the high volatility of the solutions made the aerosol evaporation to be significant already at room temperature.

Regarding LODs, it was noticed that they were higher as compared to those previously shown in section 3.2.1. This was likely a combination of the lower sensitivity and the higher background standard deviation in the case of continuous sample introduction. Nonetheless, it was verified that, also in this mode, hTISIS improved LODs as compared to double pass spray chamber for all the tested isotopes. At a 300°C heating temperature the average LOD improvement factor was close to 6.

3.3. Matrix effects caused by ethanol

3.3.1. Air-segmented injection mode

In order to evaluate the extent of non spectral interferences, the relative intensity (I_{rel}) was obtained as the ratio between the peak height obtained for a given solution and

that measured when the ethanol content was 50% (v/v). This relative parameter gave a quick indication of the extent of matrix effects. Thus interferences caused I_{rel} to deviate from 1. Figure 3 plots the obtained results as a function of the hTISIS temperature for water and the 25% ethanol solution. It was clearly observed that I_{rel} values below 1 were obtained when the chamber temperature was lower than around 150°C and 100°C for water and 25% (v/v) ethanol, respectively. Beyond these temperatures, the sensitivity for the reference solution (50% ethanol, v/v) was lower than for the other two matrices (I_{rel} higher than 1). In other words, in contrast to the findings made in ICP-OES [17], there was not a temperature at which ICP-MS interferences caused by ethanol were fully eliminated. An increase in the hTISIS temperature reduced the extent of the ethanol interference with respect to water from about 60% ($I_{rel} = 0.4$) at room temperature to 30% ($I_{rel} = 1.3$) at 300°C. Conversely, for 25% (v/v) ethanol, the matrix effects were exacerbated as increased the hTISIS temperature up to 200 – 400°C. These trends were independent of the isotope considered.

The results summarized in Figure 3 could not be explained in terms of a modification in the aerosol transport towards the plasma as either the temperature or the ethanol content were varied, because, as Figure 1 revealed these effects were alleviated using the hTISIS at high temperatures. Therefore, the reason for this trend appeared to be located at the plasma or the interface.

Doubly charged ions and oxide ratios are indicators of the plasma thermal state [20]. It was interesting to notice that, for aqueous solutions, an increase in the hTISIS temperature did not modify the double charges ratio (Figure 4.a) likely because of the so low liquid sample volume injected. Furthermore, for a given sample introduction

system and operating conditions, ethanol had a positive impact on the $^{140}\text{Ce}^{++}/^{140}\text{Ce}^{+}$ ratio. In other words, apparently this alcohol slightly improved the plasma thermal state with respect to plain water solutions. Therefore, changes in the plasma properties could not account for the behavior discussed in Figure 3. As regards oxides, heating of the hTISIS spray chamber led to minor increases in the $^{140}\text{Ce}^{16}\text{O}^{+}/^{140}\text{Ce}^{+}$ ratio (Figure 4.b). This magnitude was kept at rather low levels what expectedly did not induce significant spectral interferences.

3.3.2. Continuous sample aspiration mode

In continuous mode, as in air-segmented injection mode, non spectral interferences caused by the presence of ethanol were assessed by calculating the signal found for a given analyte and solution divided by that encountered for the 50% (v/v) ethanol standard (*i.e.*, relative intensity, I_{rel}). The results are plotted for four different chamber temperatures (Figure 5). It was found that, at room temperature, a 50% (v/v) ethanol concentration afforded two times higher signals with respect to water. Meanwhile, the increase in ethanol content from 25 to 50% (v/v) only induced a 10-20% signal increase. These results clearly showed that the introduction of this alcohol at low flow rates resulted beneficial from the point of view of sensitivity. Interestingly, when the chamber temperature was increased to 150°C, an increase in ethanol content from 25 to 50% (v/v) induced a drop in sensitivity ($I_{\text{rel}} > 1$) whereas the matrix effect was mitigated with respect to room temperature (relative intensities were closer to 1 at 150°C than with no heating). A similar situation was found when heating the chamber at 300°C and, finally, at 400°C even water provided higher sensitivities than the 50%

(v/v) ethanol standard. In other words, a negative interference was caused by ethanol when the highest temperature was evaluated. The trend was similar for almost all the analytes, except Ag, Ba, Bi, Ag and Pb that showed cross-over points at lower temperatures than for the rest of the analytes. All these trends were identical as those found when the sample was delivered to the nebulizer as discrete plugs (see Figure 3).

3.3.3. Possible explanation of the observed matrix effects

Apparently, the observed non spectral interferences were related with neither the sample introduction system nor the plasma thermal state. Therefore, they were expected to be caused by a modification in the ion sampling efficiency. The basic idea was to consider that, in presence of ethanol and at high hTISIS temperatures, aerosol droplets evaporated either inside the chamber or at the plasma base. As a result, analyte ions were generated close to the coil (upstream the plasma) in presence of ethanol and/or at high temperatures thus giving rise to a higher likelihood for ionic plasma radial diffusion. Therefore, the ionic spatial distribution inside the plasma was a function of both hTISIS temperature and ethanol concentration. In order to verify this hypothesis, the ionic signals were taken at different plasma – sampling cone relative positions for both sample air-segmented (Figure 6.a) and continuous (Figure 6.b) aspiration at different ethanol contents and hTISIS temperatures. The obtained results are included in Figure 6 for ^{55}Mn and show that the obtained bell shaped signal profiles appeared off plasma axis. At room temperature, the curves for the solutions containing 25% and 50% of ethanol were located at virtually the same intensity levels. Meanwhile water afforded lower intensities for all the evaluated positions. When the

hTISIS chamber was heated, the three profiles approached although the value of the maximum ionic signal depended on the matrix. In order to remove the effect, it was necessary to move the torch position about 1 mm plasma down axis. Under these circumstances, the sensitivity was not dependent on the ethanol content and it was possible to perform elemental quantification through external calibration employing 1:1 ethanol:water standards. The obvious consequence of this procedure was that sensitivity decreased by a factor close to 20% in discrete mode (Figure 6.a) and 40% in continuous mode (Figure 6.b) as compared to the maximum achievable signal. However, the LODs were not degraded as compared with those obtained at room temperature (Table 2). All these observations were not dependent of the analyte m/z ratio.

Sampling depth profiles were also acquired and are outlined in Figure 7 in order to verify the observed trends in terms of radial profiles. The results are summarized for the continuous sample introduction mode. It was noticed that at room temperature, ethanol solutions provided higher ionic counting than water. A maximum in sensitivity was registered when the signal was taken at a 5 mm sampling depth. However, as the hTISIS chamber temperature was increased up to 300°C, the profiles for the three solutions evaluated were located at virtually the same positions. Interestingly no maxima in ionic signal were found. This later observation was compatible with the idea that an increase in the chamber temperature led to an analyte ionization upstream the plasma. These experiments revealed that the interferences caused by ethanol could also be corrected for by setting the sampling depth at 3 mm. However, the standard deviation for the blanks was also higher than when the sampling depth was set at 10

mm and the torch moved 1 mm plasma down axis. As a consequence, the LODs were similar to or higher than those shown in Table 2.

3.4. Recovery tests

Four bioethanol real samples, spiked with a multielemental solution, were analyzed under the optimized hTISIS operating conditions through external calibration employing 50% ethanol standards. The samples were selected based on their different water content and, hence, possibility to cause matrix effects. The recovery tests were performed in both aspiration modes. As Figure 8 demonstrates, good results (*i.e.*, recoveries close to 100%) were generally obtained.

As an alternative procedure to the recovery tests, bioethanol samples were preconcentrated. Thus, 40 mL bioethanol sample volumes were allowed to completely evaporate for 24 h in a hood at room temperature. Once this step was completed, the solid residue was dissolved by adding 8 mL of either ethanol or water. The solutions were sonicated for 5 min and analyzed through both ICP-MS and ICP-OES. The obtained results were compared against those found with the hTISIS through external calibration with 1:1 ethanol:water standards. Figure 9 reveals that the five methodologies evaluated employing direct analysis or preconcentration, ethanol or water dissolution, ICP-OES [17] or ICP-MS, provided similar concentrations. These results give a proof of the hTISIS suitability for performing direct bioethanol analysis.

3.5. Analysis of bioethanol real samples

A set of 28 bioethanol real samples were analyzed by means of the hTISIS under both continuous and discrete sample introduction modes. All the obtained concentrations together with the confidence intervals ($n=5$ and $\alpha=0.05$) are summarized in Table 3. An external calibration approach using ethanol:water (1:1 v/v) standards was applied. Only the elements found at concentrations above the limits of quantification ($LOQ = 10 LOD/3$) are considered. Sodium and Magnesium were found as major analytes in the bioethanol samples. The sources of these elements may vary from sample to sample. Furthermore, they can be externally incorporated to the final product. Indeed, in the particular case of sodium, preliminary experiments have demonstrated that it may migrate from glass components and hence accumulate in bioethanol samples. In contrast, trace elements (Ag, Ba, Co, Cu, Fe, Mn, Ni, Sr and Zn) were found at levels above the LOQ only for some samples.

The found concentrations in bioethanol real samples gathered in Table 3 were of the same order as those previously reported in the literature [6]. Thus, Cr, Cu, Fe, Mn and Ni were found by other authors in the tens of ppb range whereas the highest concentrations quantified in the present work were 21, 30, 171, 15 and 29 $ng mL^{-1}$, respectively. Besides these elements, Mg, Na and Zn were found at levels on the order of several hundreds of ppb in previous reports. In the present work, they were quantified at tens to hundreds of ppb. Finally, trace analytes as Ag, Al, Cd, Co, Sr and Pb have been hardly found in the literature because their concentrations are below the LOD. In this work, these analytes were quantified at the sub-ppb level. Obviously, the found concentrations reported for some analytes in ethanol-fuel samples was above those obtained in the present work. Note that ethanol-fuel samples correspond to

bioethanol-gasoline blends and some analytes mainly come from gasoline. For instance, Pb was found by Neves *et al.* [16] at tens of ppb in ethanol-fuel samples whereas, in the present work, this element has been found at levels below 1.5 ng mL^{-1} in bioethanol samples.

4. Conclusions

The use of the hTISIS for the direct bioethanol elemental analysis through ICP-MS provides sensitive and accurate results. This assessment is based on the fact that, at high temperatures, the analyte transport related interferences caused by ethanol are removed. Therefore, it is possible to apply an external calibration approach in which ethanol:water (1:1 v/v) standards are used. Furthermore, the hTISIS provides higher sensitivities and lower limits of detection than a conventional sample introduction system. This result is extremely interesting for samples such as bioethanol in which the analytes are present at actually low concentrations.

The obtained results also demonstrate that the operating conditions should be optimized in terms of accuracy instead of sensitivity. In fact, it has been necessary to vertically modify the plasma position to find the zone at which the sensitivity does not depend on the ethanol content. This modification involves a drop in sensitivity with respect to the centered position that can be as high as 40%. Fortunately, the hTISIS is able to improve this parameter by a factor going from 4 to 8 as compared to a conventional device.

Acknowledgements

The authors wish to acknowledge G. Coleman (Meinhard Glass Products) for the loan of the nebulizer employed in the present study, the IFPEN for the financial support and samples delivered and the UNGDA for the samples provided to carry out this work. C. Sánchez would like to thank the Ministry of Education, Culture and Sports, Spain for the grant FPU 13/01438.

5. References

-
- [1] H. Habe, T. Shinbo, T. Yamamoto, S. Sato, H. Shimada, and K. Sakaki, Chemical Analysis of impurities in diverse bioethanol samples, *J. Japan Pet. Inst.*, 56 (2013) 414–422.
 - [2] G. M. Walker, *Bioethanol: Science and technology of fuel alcohol*, Ventus Publishing ApS, 2010.
 - [3] D. Chiche, C. Diverchy, A. C. Lucquin, F. Porcheron, and F. Defoort, Synthesis gas purification, *Oil Gas Sci. Technol. – Rev. d'IFP Energies Nouv.*, 68 (2013) 707–723.
 - [4] AMERICAN SOCIETY FOR TESTING MATERIALS – ASTM D4806 – Standard Specification for Denatured Fuel Ethanol for Blending with Gasolines for Use as Automotive Spark-Ignition Engine Fuel.
 - [5] ASSOCIACAO BRASILEIRA DE NORMAS TECNICAS – ABNT NBR 11331- Ethyl alcohol – Determination of iron and copper concentrations – Atomic absorption spectrophotometry method.

- [6] R. Sánchez, C. Sánchez, C.-P. Lienemann, and J.-L. Todolí, Metal and metalloid determination in biodiesel and bioethanol, *J. Anal. At. Spectrom.*, 30 (2015) 64–101.
- [7] C.C. Leite, A. de Jesus, M.L. Potes, M.A. Vieira, D. Samios, M.M. Silva, Direct determination of Cd, Co, Cu, Fe, Mn, Na, Ni, Pb and Zn in ethanol fuel by high resolution continuum source flame atomic absorption spectrometry, *Energy Fuels*, 29 (2015) 7358-7363.
- [8] M. Ben-Younes, D.C. Gregoire, C.L. Chakrabarti, Effectiveness of ammonia in reducing carbon-based polyatomic ion interferences in electrothermal vaporization collision cell inductively coupled plasma mass spectrometry, *Spectrochim. Acta Part B*, 2003, 58, 361–372
- [9] D.R. Neves, R.S. Amais, J.A. Nobrega, J.A. Gomes Neto, Assessment of Polyatomic Interferences Elimination Using a Collision Reaction Interface (CRI) for Inorganic Analysis of Fuel Ethanol by ICP-QMS, *Anal. Letters*, 2012, 45, 1111–1121.
- [10] T.D. Saint’Pierre, T.A. Maranhao, V.L.A. Frescura, A.J. Curtius, *Spectrochim. Acta, Part B*, The development of a method for the determination of trace elements in fuel alcohol by electrothermal vaporization–inductively coupled plasma mass spectrometry using external calibration, 2005, 60, 605– 613.
- [11] L. Tormen E.S. Chaves, T.D. Saint’Pierre, V.L.A. Frescura, A.J. Curtius, *J. Anal. At. Spectrom.*, Determination of trace elements in fuel ethanol by ICP-MS using direct sample introduction by a microconcentric nebulizer, 2008, 23, 1300–1304.

- [12] T.D. Saint’Pierre, L. Tormen, V.L.A. Frescura, A.J. Curtius, *J. Anal. At. Spectrom.*, The direct analysis of fuel ethanol by ICP-MS using a flow injection system coupled to an ultrasonic nebulizer for sample introduction, 2006, 21, 1340–1344.
- [13] A. Virgilio, R.S. Amais, D. Schiavo, J.A. Nóbrega, Dilute-and-Shoot Procedure for Determination of As, Cr, P, Pb, Si, and V in Ethanol Fuel by Inductively Coupled Plasma Tandem Mass Spectrometry, *Energy Fuels*, 2015, 29, 4339–4344.
- [14] E. McCurdy and D. Potter, *Techniques for the Analysis of Organic Chemicals by Inductively Coupled Plasma Mass Spectrometry (ICP-MS)*, *Agil. Technol.*, 1 (2002) 5988-6190E.
- [15] M. S. Rocha, M. F. Mesko, F. F. Silva, R. C. Sena, M. C. B. Quaresma, T. O. Araújo, and L. A. Reis, Determination of Cu and Fe in fuel ethanol by ICP OES using direct sample introduction by an ultrasonic nebulizer and membrane desolvator, *J. Anal. At. Spectrom.*, 2011, 26, 456-461.
- [16] D. R. Neves, R. S. Amais, J. A. Nóbrega, J. A. G. Neto, Assessment of Polyatomic Interferences Elimination Using a Collision Reaction Interface (CRI) for Inorganic Analysis of Fuel Ethanol by ICP-QMS, *Anal. Lett.*, 2012, 45, 1111–1121.
- [17] C. Sánchez, C.P. Lienemann, J.L. Todolí, Metals and metalloids determination in bioethanol through ICP-OES, *Spectrochim. Acta, Part B*, 115 (2016) 16-22.
- [18] R. Sánchez, C. Sánchez, J.L. Todolí, C.P. Lienemann, J.M. Mermet, Quantification of nickel, vanadium and manganese in petroleum products and biofuels through inductively coupled plasma mass spectrometry equipped with a high

-
- temperature single pass spray chamber, *J. Anal. At. Spectrom.*, 2014, 29, 242-248
- [19] R. Sánchez, J.L. Todolí, C.P. Lienemann, J.M. Mermet, Universal calibration for metal determination in fuels and biofuels by inductively coupled plasma atomic emission spectrometry based on segmented flow injection and a 350 °C heated chamber, *J. Anal. At. Spectrom.*, 2012, 27, 937-945.
- [20] Y. Makonnen, D. Beauchemin, Investigation of a measure of robustness in inductively coupled plasma mass spectrometry, *Spectrochim. Acta, Part B*, 103–104 (2015) 57–62.

Table 1. ICP-MS Agilent 7700x operating conditions.

Plasma			
Ar flow rates/L min ⁻¹	Plasma gas: 15.0		
RF power/W	Auxiliary gas: 0.9		
	1600		
htISIS conditions			
Sample injection mode	Air Segmented injection	Continuous sample aspiration	
Volume injected/ μ L	5	-----	
Liquid aspiration conditions	350 rpm (air)	25 μ L min ⁻¹	
Nebulization flow rate/ L min ⁻¹		0.4	
Number of replicates		5	
Integration software	Transient (TRA)	Spectrum	
Integration time/s	0.1	0.3	
Sweeps per replicate	1	100	
Total acquisition time/s	300 s (for 5 peaks)	-----	
Collision cell			
He flow rate/mL min ⁻¹	4.3		
OctP Bias/V	-18		
Oct RF/V	200		
Energy discrimination/V	3.0		
HMI System Conditions			
Ar HMI flow rate/ L min ⁻¹	0.56		
Measured isotopes			
⁷ Li	¹¹ B	⁴³ Ca	⁴⁴ Ca
²⁷ Al	⁵⁵ Mn	⁵⁶ Fe	⁶⁰ Ni
⁵² Cr	⁶⁶ Zn	⁷⁵ As	⁸⁸ Sr
⁶³ Cu	¹¹¹ Cd	¹¹⁵ In	¹³⁶ Ba
¹⁰⁷ Ag	¹⁴⁰ Ce	²⁰⁸ Pb	²⁰⁹ Bi
¹³⁷ Ba	¹⁵⁶ CeO ⁺	⁶⁸ Ba ²⁺	⁷⁰ Ce ²⁺
¹⁵⁴ BaO ⁺	²³ Na	²⁴ Mg	

Table 2. Limits of detection for 50% ethanol/water mixtures and different sample introduction systems in air segmented injection mode.

LODs (ng/mL)			
Isotope	Double pass	hTISIS Room temperature	hTISIS 300°C
¹¹ B	34	2	3
²³ Na	7	4	5
²⁴ Mg	1.1	1.3	0.6
²⁷ Al	3	3	3
⁵² Cr	0.4	0.3	0.17
⁵⁵ Mn	0.4	0.2	0.2
⁵⁶ Fe	0.5	0.5	0.4
⁵⁹ Co	0.3	0.04	0.014
⁶⁰ Ni	0.6	0.11	0.06
⁶³ Cu	0.3	0.11	0.17
⁶⁶ Zn	0.18	0.08	0.05
⁸⁸ Sr	0.3	0.06	0.05
¹⁰⁷ Ag	0.17	0.04	0.015
¹¹¹ Cd	0.3	n.a.	0.2
¹¹⁵ In	0.12	0.08	0.03
¹³⁷ Ba	0.3	n.a.	0.04
²⁰⁸ Pb	0.3	0.03	0.018

^{209}Bi	0.13	0.018	0.019
-------------------	------	-------	-------

Table 3. Found concentrations (in ng mL^{-1}) in real bioethanol samples by means of the hTISIS-ICP-MS in continuous aspiration (CA).*

Sample	Analyte	Concentration	Sample	Analyte	Concentration	
B1	Na	792 ± 50	B10	Co	1.42 ± 0.11	
	Fe	11.5 ± 0.7		Ni	6.4 ± 0.8	
	Co	2.2 ± 0.2		Ag	1.16 ± 0.09	
	B2	Ni	3.8 ± 0.5	B11	Na	903 ± 31
		Cu	14.3 ± 1.5		Fe	6.3 ± 1.8
		Zn	830 ± 49		Co	1.12 ± 0.09
		In	10.1 ± 0.7		Ni	5.2 ± 0.5
B3		Na	1909 ± 795	Ag	1.10 ± 0.09	
		Mg	< LOQ	B12	Na	872 ± 33
	Fe	5.9 ± 0.5	Fe		5.8 ± 0.7	
	Co	1.70 ± 0.09	Co		1.26 ± 0.16	
	Ni	2.9 ± 0.4	Ni		4.7 ± 0.3	
	Ag	4.1 ± 0.2	Ag		1.21 ± 0.08	
B4	Na	970 ± 42	B13	Na	804 ± 32	
	Fe	6.2 ± 0.3		Fe	6.1 ± 0.5	
	Co	1.5 ± 0.2		Co	1.71 ± 0.17	
	Ag	2.19 ± 0.14		Ni	4.1 ± 0.4	
B5	Na	626 ± 33	Ag	1.30 ± 0.06		
	Fe	7.2 ± 0.7	B14	Na	883 ± 32	
	Co	2.5 ± 0.2		Fe	6.2 ± 0.4	
	Ni	4.0 ± 0.5		Co	1.8 ± 0.2	
	Cu	15.4 ± 0.9		Ag	1.26 ± 0.16	
	B6	Ag	10.3 ± 0.5	B15	Na	824 ± 27
Na		1760 ± 52	Fe		5.4 ± 0.5	
Mn		14.9 ± 0.8	Co		1.70 ± 0.17	
Fe		8.4 ± 1.4	Ni		4.2 ± 0.2	
Co		1.06 ± 0.12	Ag		1.20 ± 0.07	
B7	Cu	21.4 ± 1.9	B16	Na	1776 ± 268	
	Na	271 ± 34		Fe	6.5 ± 1.7	
				Co	1.9 ± 0.3	
				Ni	5.3 ± 0.3	
		Cu		13.6 ± 1.6		

	Mg	< LOQ			Ag	1.40 ± 0.05	
	Fe	5.2 ± 0.2		B17	Na	621 ± 36	
	Co	1.23 ± 0.15			Ag	2.06 ± 0.17	
	Ni	3.4 ± 0.2					
	Ag	2.08 ± 0.16					
Table 3 (continued)							
B7	Na	295 ± 39		B18	Na	471 ± 22	
	Fe	11 ± 6			Ag	1.9 ± 0.6	
	Co	1.10 ± 0.14		B19	Na	639 ± 10	
	Ni	21.1 ± 0.8		B20	Na	979 ± 16	
	Cu	35.7 ± 1.5			B21	Na	429 ± 17
	Zn	145 ± 9			B22	Na	488 ± 22
	Ag	3.4 ± 0.3		B23	Na	560 ± 13	
B8	Na	490 ± 24	B24	Na	493 ± 15		
	Fe	11.7 ± 0.4	B25	Na	272 ± 13		
	Co	2.9 ± 0.4	B26	Na	347 ± 12		
	Ni	3.9 ± 0.2	B27	Na	884 ± 18		
	Cu	23.8 ± 1.9	B28	Na	1832 ± 47		
	Sr	1.7 ± 0.4		Mn	4.4 ± 0.5		
	Ag	18.3 ± 1.8		Fe	171 ± 17		
In	13.5 ± 0.5	Ni		29.3 ± 0.6			
B9	Na	1203 ± 192	Ag	15 ± 3			
	Cr	21 ± 2					
	Fe	37 ± 47					
	Co	1.19 ± 0.08					
	Ni	10.4 ± 1.1					
	Cu	14.8 ± 0.9					
	Ag	1.65 ± 0.10					
B10	Na	1176 ± 78					
	Fe	7.0 ± 1.9					

*Confidence intervals (n=5 and $\alpha=0.05$).

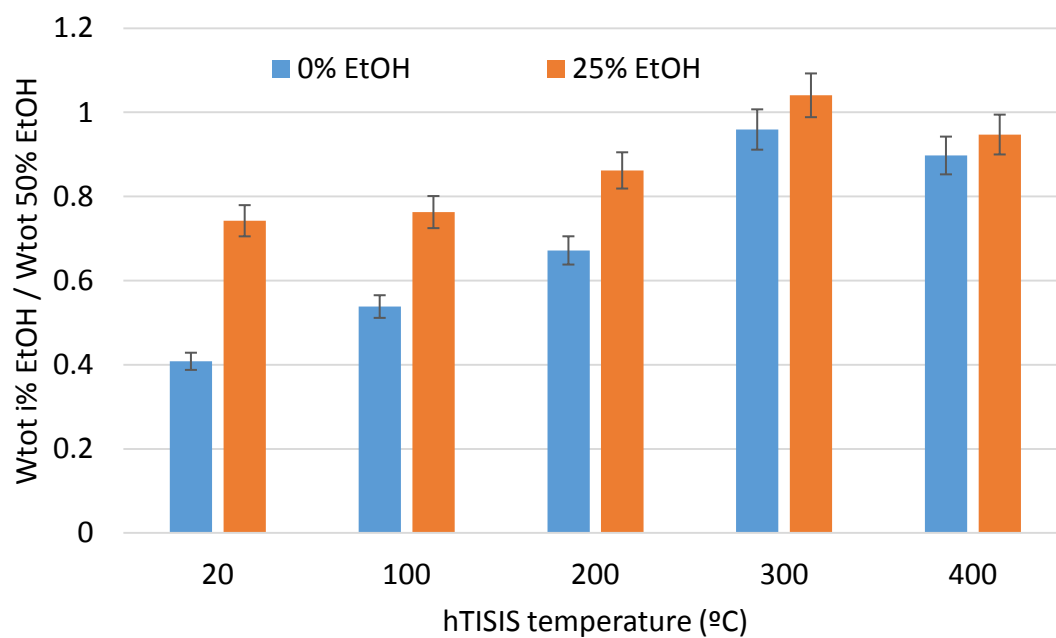


Figure 1. Analyte mass leaving the spray chamber per unit of time (W_{tot}) normalized with respect to that measured when the ethanol concentration is 50% versus hTISIS temperature.

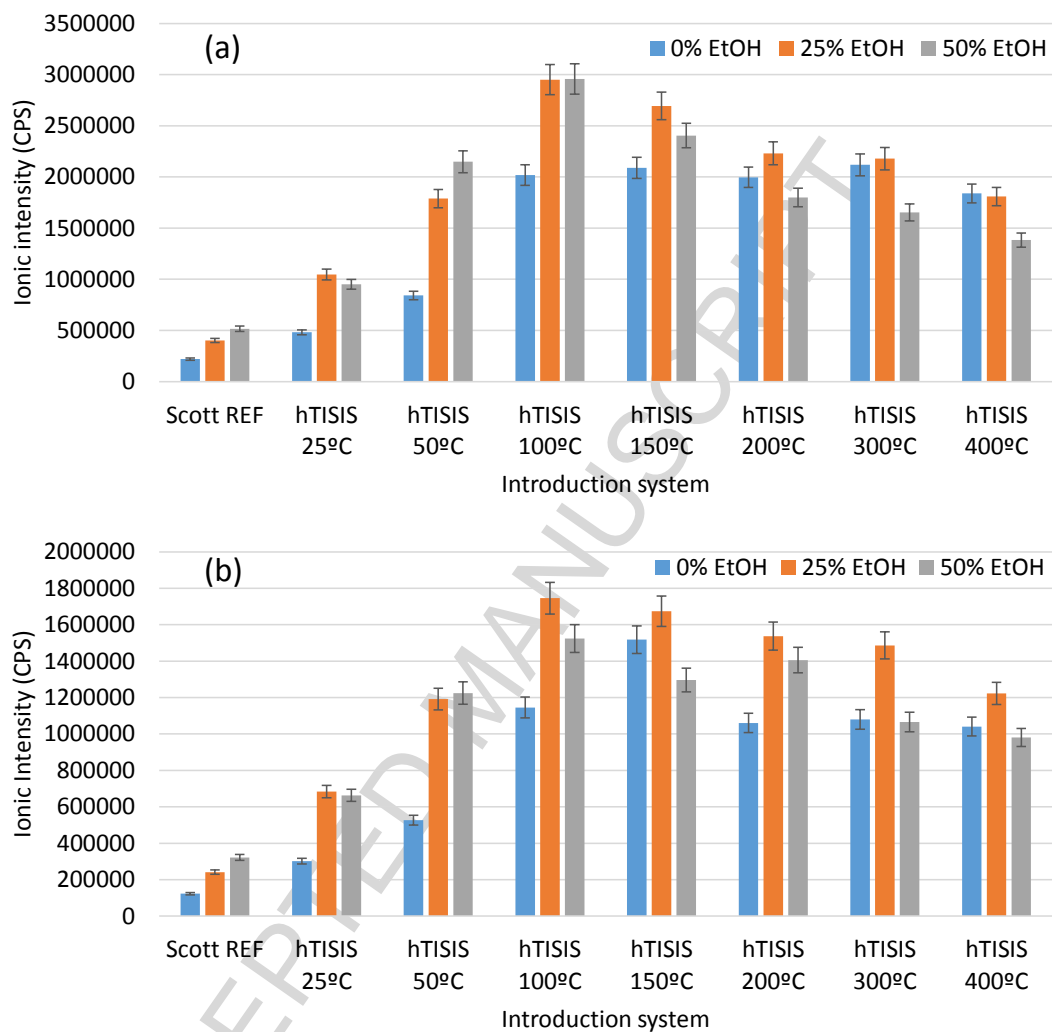


Figure 2. Effect of the sample introduction system and hTISIS temperature on the signal (taken as peak height). (a) ^{55}Mn ; (b) ^{111}Cd .

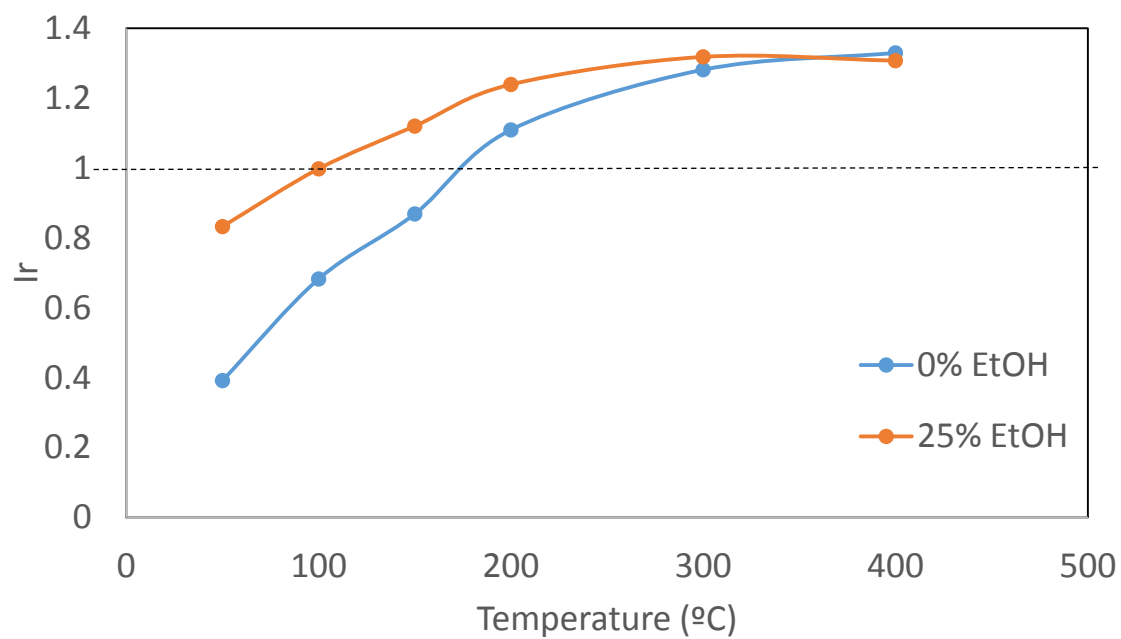


Figure 3. Relative intensity variation (taking the 50% ethanol solution as reference) versus the hTISIS temperature for two different matrices under the air-segmented injection mode. Isotope: ^{55}Mn .

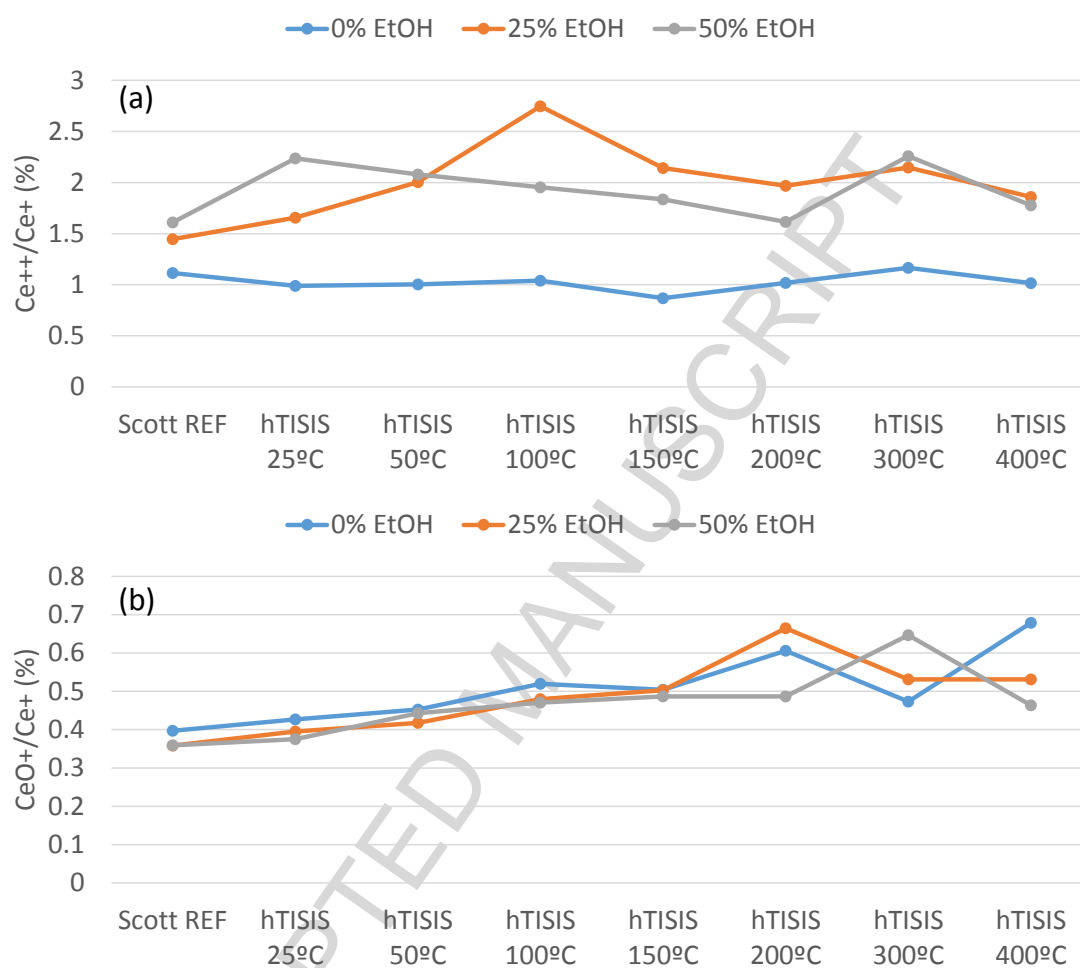


Figure 4. Doubly charged ion (a) and oxide ratios (b) for the two sample introduction systems and several hTISIS temperatures. Air segmented mode.

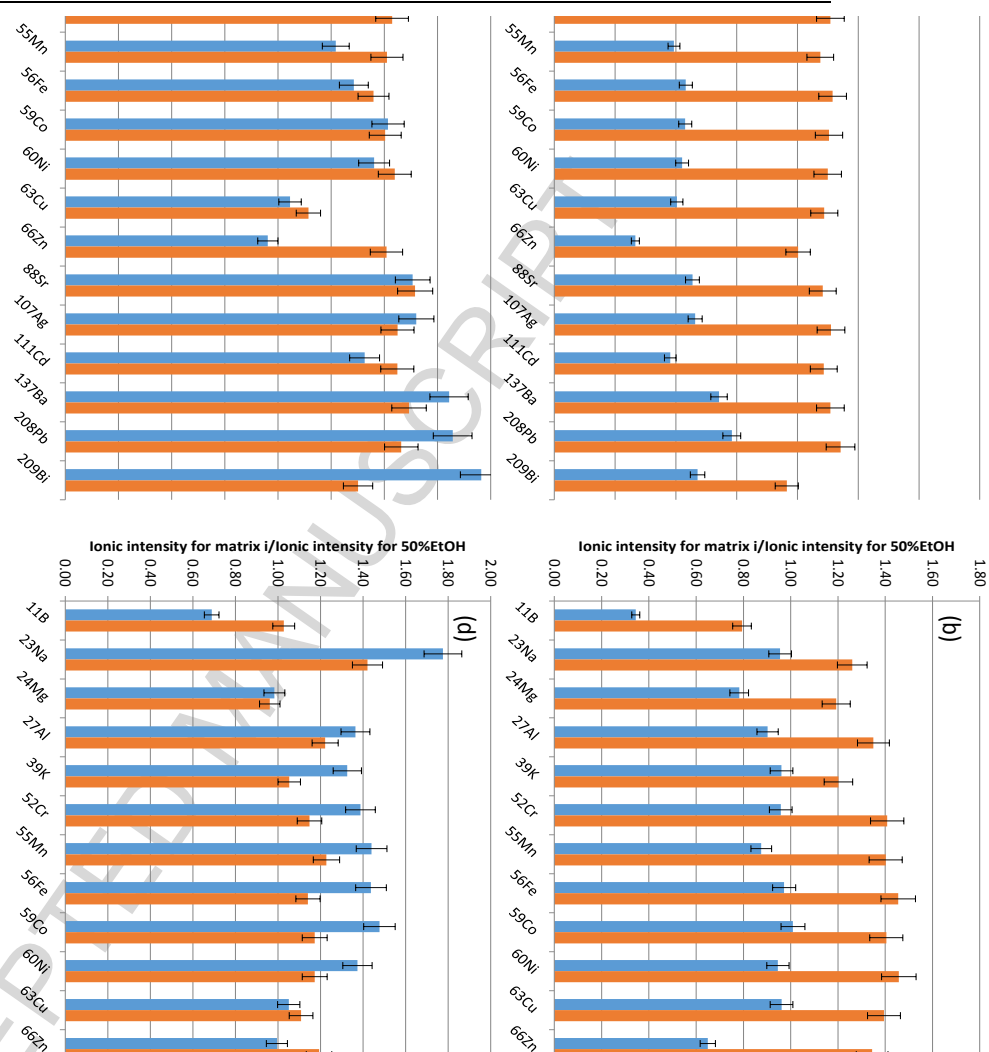


Figure 5. Effect of the chamber walls temperature on the extent of matrix effects. Blue bars: 0% EtOH; orange bars: 25% EtOH (v/v). (a) Room temperature; (b) 150°C; (c) 300°C; (d) 400°C.

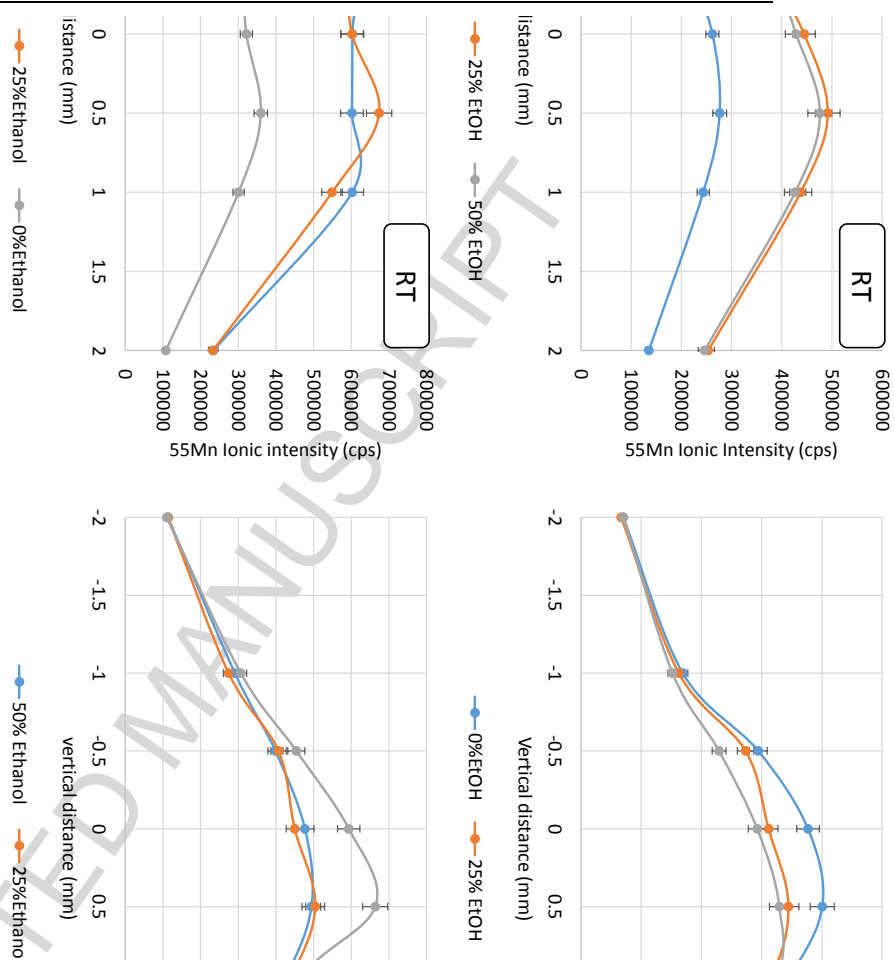


Figure 6. ICP-MS radial plasma profiles obtained for two different temperatures and three different solutions. (a) Air-segmented mode; (b) Continuous mode. Sampling depth 10 mm. Isotope: ^{55}Mn .

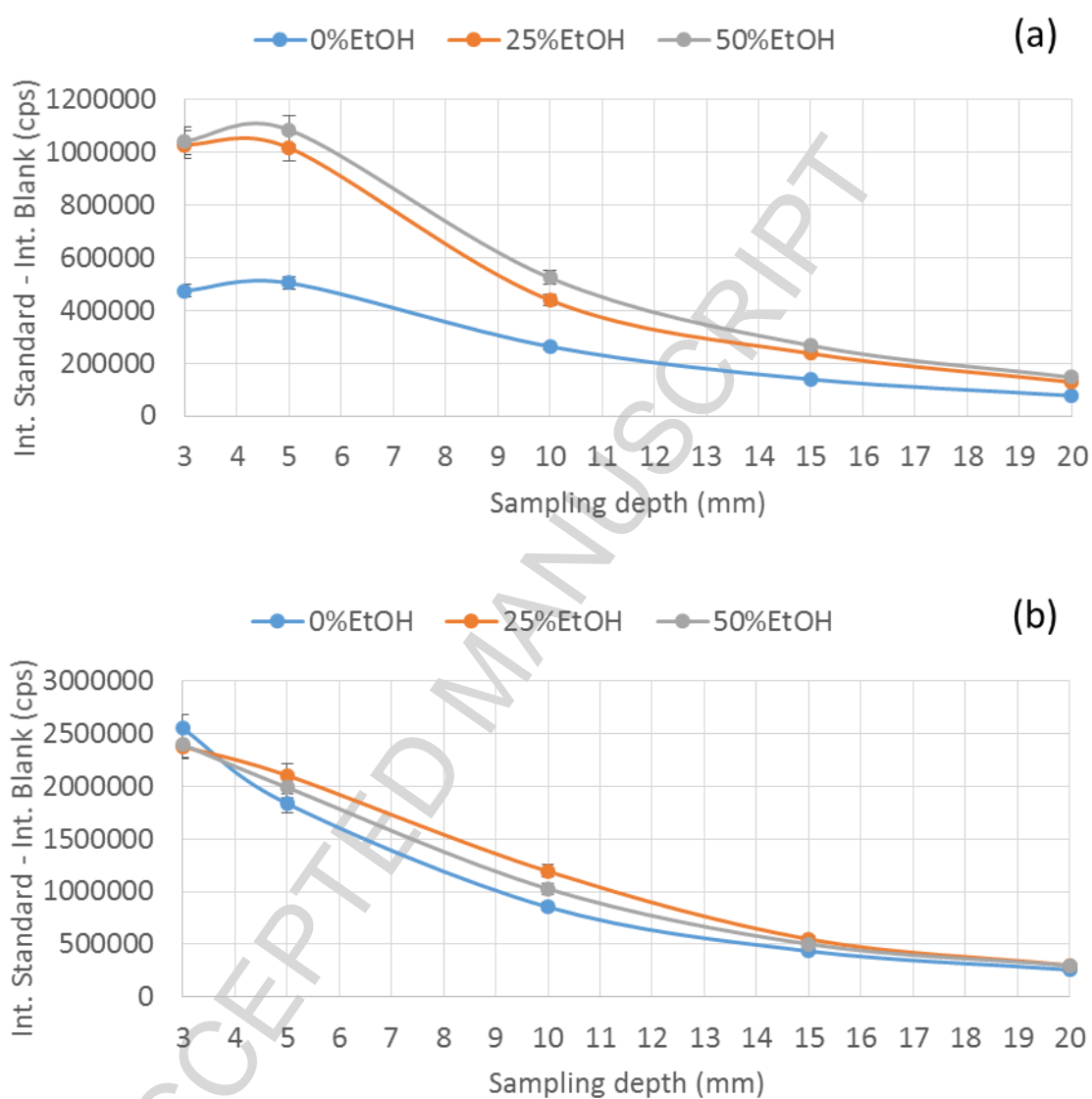


Figure 7. ICP-MS axial plasma profiles obtained for two different temperatures and three different solutions. (a) Room temperature; (b) 300°C heating temperature.

Vertical torch position 0 mm. Isotope: ^{55}Mn .

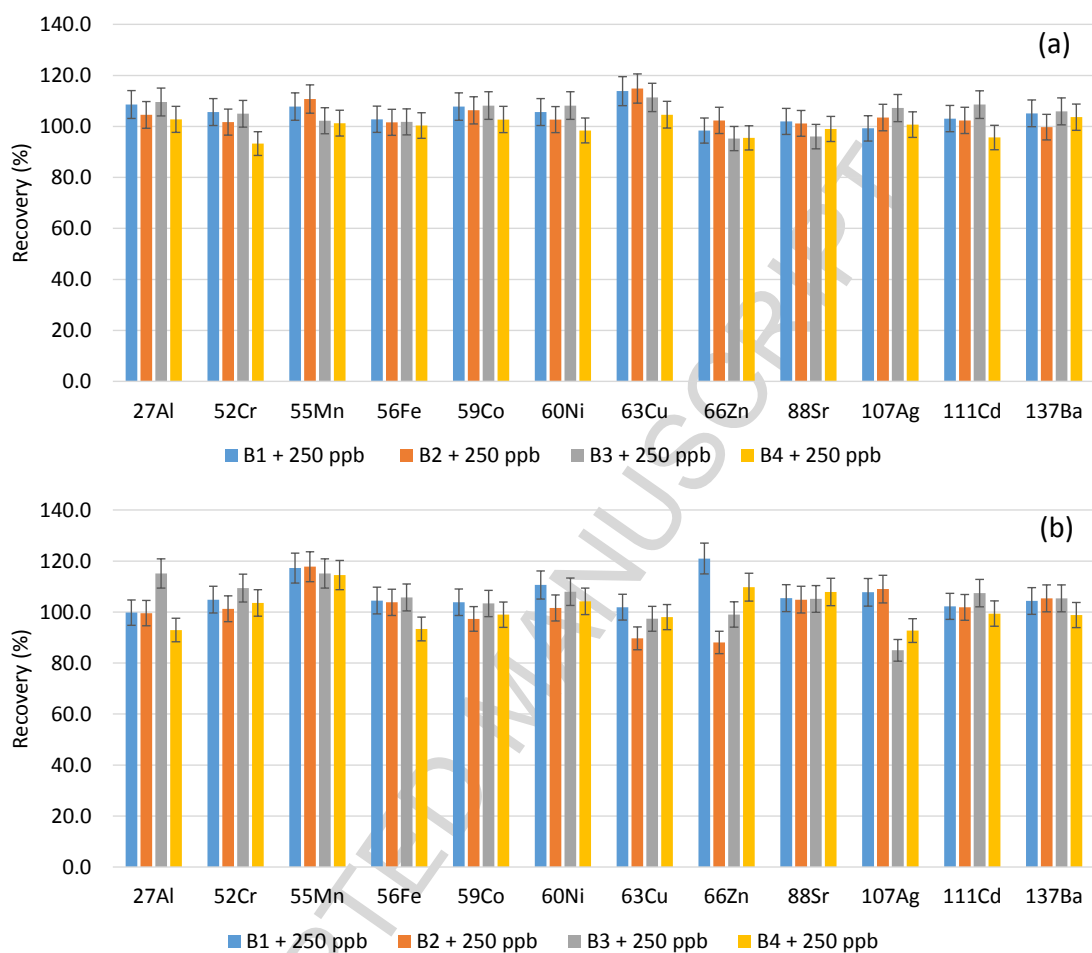


Figure 8. Recoveries found for four real bioethanol spiked samples (250 mg L^{-1}) under air-segmented (a) and continuous aspiration (b) modes. hTISIS temperature: 300°C , Plasma vertical distance: -1 mm ; sampling depth: 10 mm . B1 Anhydrous bioethanol; B3: Anhydrous ethanol with additives; B2 and B4: hydrated bioethanol.

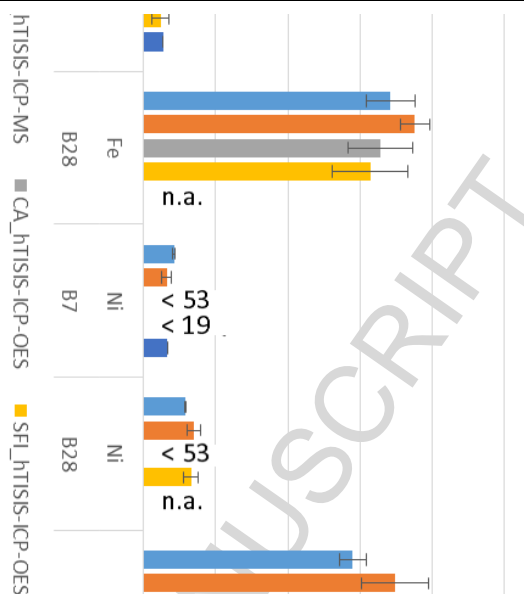


Figure 9. Elemental concentrations found for several bioethanol samples following five different procedures. CA: Continuous aspiration; SFI: Segmented flow injection.

Graphical abstract

A high temperature torch integrated sample introduction system (hTISIS) has been employed to carry out analysis of bioethanol samples through ICP-MS

Ethanol interferences can be removed by both optimizing the hTISIS temperature and modifying the torch position with respect to the spectrometer interface

Accurate results have been obtained with a single set of calibration standards for samples containing different ethanol content

Highlights

The aerosol heating leads to an increase in the ICP-MS sensitivity and a lowering in the detection limits for ethanol containing samples

Ionic spatial distribution inside the plasma depends on both the aerosol temperature and ethanol concentration

Aerosol heating together with a modification of the torch position yield accurate results